Journal of Applied Mechanics and Technical Physics, Vol. 48, No. 5, pp. 712–722, 2007

DYNAMIC DEFORMATION OF RIGID-PLASTIC CURVILINEAR PLATES OF VARIABLE THICKNESS

Yu. V. Nemirovsky and T. P. Romanova

UDC 539.4+539.37

A general solution is obtained for the problem of dynamic bending of an ideal rigid-plastic plate of variable thickness with a simply supported or clamped curvilinear contour under the action of a short-time high-intensity explosive-type load uniformly distributed over the surface. Several mechanisms of plate deformation are demonstrated to exist. For each mechanism, equations of dynamic deformation are derived and conditions of mechanism implementation are analyzed. Examples of numerical solutions are given.

Key words: *rigid-plastic plate, curvilinear contour, variable thickness, dynamic load, limit load, final deflection.*

Introduction. Studying the dynamic behavior of structural elements under explosive loading is extremely important for estimating the degree of structural damage, analyzing the risks, and predicting emergency situations. The model of an ideal rigid-plastic body is widely used to solve problems of this type [1]. Based on this model, the dynamic behavior of curvilinear plates of constant thickness under dynamic loading was examined in [2–9].

The most important task in creating shields protecting from explosive loads is the choice of the material and its distribution in the structure providing the minimum degree of damaging. This problem is directly related to optimal design, which has been fairly well studied, as applied to static and dynamic harmonic actions on various structures [10, 11]. The necessity of solving problems of structural optimization under dynamic loading has been intensely discussed in the literature [12]. Nevertheless, we are unaware of any research in this field, except for beams [13] and shells of revolution [14]. The present paper continues the research in this field, as applied to flat plates with a complicated convex support contour.

A method based on the model of an ideal rigid-plastic body is proposed in the paper. This method allows one to calculate curvilinear plates of variable thickness of a certain type under the action of short-time high-intensity dynamic loads. The method can be used for various engineering calculations.

1. Let us consider a thin ideal rigid-plastic plate of variable thickness with a curvilinear contour, which is simply supported or clamped. The plate is subjected to an explosive load uniformly distributed over the surface. The load has an intensity $P(t)$, which instantaneously reaches the maximum value $P_{\max} = P(0)$ at the initial time $t = 0$ and then rapidly decreases. The plate has an arbitrary piecewise-smooth convex contour l defined in a parametric form as $x = x_1(\varphi)$, $y = y_1(\varphi)$, $0 \leqslant \varphi \leqslant 2\pi$. The radius of curvature of the contour l (except for singular points) is

$$R(\varphi) = L^3(\varphi)/(x_1' y_1'' - x_1'' y_1').$$

Here $L(\varphi) = \sqrt{x_1'^2(\varphi) + y_1'^2(\varphi)}$ and $(\,\cdot\,)' = \partial(\,\cdot\,)/\partial\varphi$. For certainty, we consider plates symmetric with respect to the x axis; the geometric size of the plate in the y direction is not greater than its x size; singular points of the contour are located on the x axis only (Fig. 1).

Khristianovich Institute of Theoretical and Applied Mechanics, Siberian Division, Russian Academy of Sciences, Novosibirsk 630090; nemirov@itam.nsc.ru. Translated from Prikladnaya Mekhanika i Tekhnicheskaya Fizika, Vol. 48, No. 5, pp. 108–120, September–October, 2007. Original article submitted October 6, 2006.

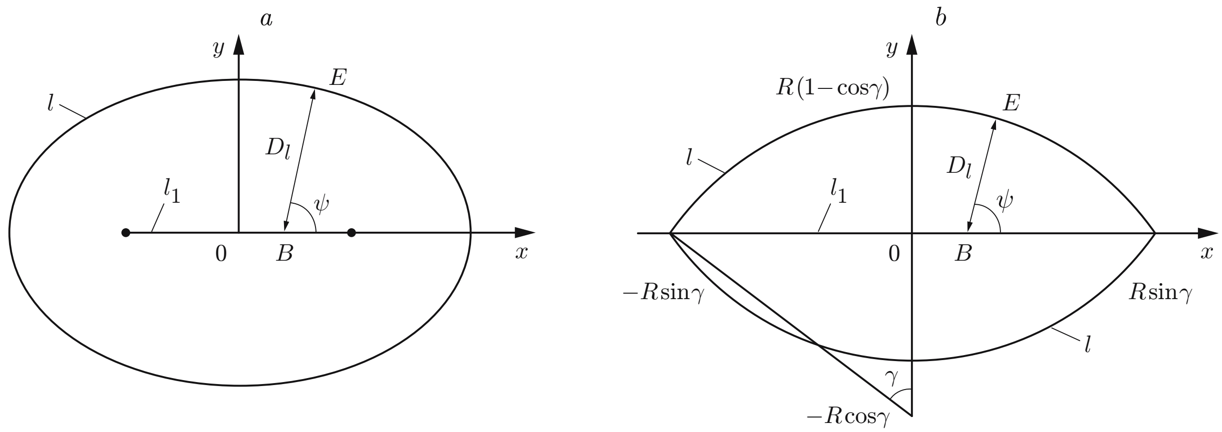

Fig. 1. Scheme No. 1 of deformation of a plate without singular points (a) and with singular points (b) on the contour.

We introduce a curvilinear orthogonal coordinate system (ν_1, ν_2) related to the Cartesian coordinate system (x, y) as

$$x = x_1(\nu_2) - \nu_1 y_1'(\nu_2)/L(\nu_2), \qquad y = y_1(\nu_2) + \nu_1 x_1'(\nu_2)/L(\nu_2).$$

The curves $\nu_1 = \text{const}$ are located at a distance ν_1 from the contour l and have a curvature radius $\rho_1 = R(\nu_2) - \nu_1$. The straight lines $\nu_2 = \text{const}$ are perpendicular to the contour l (the curvature radius is $\rho_2 = \infty$). In this case, the equation of the plate contour l has the form $\nu_1 = 0$, $0 \leqslant \nu_2 \leqslant 2\pi$.

We assume that the plate thickness h is a function of the parameter ν_1 and changes symmetrically with respect to the mid-surface of the plate. We consider the scheme of deformation of a curvilinear plate with a certain function of its thickness $h(\nu_1)$: $h(\nu_1) = \text{const}$ for $\nu_1 \geqslant \nu_1^c$ (ν_1^c is a certain prescribed value). Other restrictions on the function $h(\nu_1)$ and on the value of $P_{\max}$ are described below.

Depending on the value of $P_{\max}$, there are three possible schemes of deformation of the considered plate made of a rigid-plastic material. Under loads lower than the limit loads ("low" loads), the plate remains at rest. Under loads slightly higher than the limit loads ("medium" loads), the plate is deformed to a certain ruled surface. As in the case of a constant-thickness plate [2, 4–8], deformation of a variable-thickness plate is accompanied by formation of a line plastic hinge l_1 in the inner region of the plate. By virtue of plate symmetry, the hinge l_1 is located on the x axis. If there are singular points on the contour l, the hinge l_1 passes through these points.

Let $D_l(\nu_2)$ be the distance between the contour l and the line l_1 along the normal to l (see Fig. 1) [2]:

$$D_l(\nu_2) = |y_1(\nu_2)/x_1'(\nu_2)| L(\nu_2).$$

Then, the hinge l_1 is located in the interval $x_1(\pi) - D_l(\pi) \leqslant x \leqslant x_1(0) - D_l(0)$ and is defined by the equation

$$\nu_1 = D_l(\nu_2), \qquad 0 \leqslant \nu_2 \leqslant \pi. \tag{1}$$

The normal bending moment on the line l_1 is $\sigma_0 h^2(D_l)/4$ (σ_0 is the yield point of the plate material). Such a scheme of motion is called scheme No. 1.

As in the case of bending of beams [1], circular and annular plates, rectangular and polygonal plates [1], plates with a complex-shaped contour [2–9], dynamic deformation of a variable-thickness plate at rather high values of $P_{\max}$ may be accompanied by the emergence of a region of intense plastic deformation Z_p moving translationally. In this case, situations are possible with part of the hinge l_1 retained (scheme No. 2) or with the hinge l_1 absent (scheme No. 3). Scheme No. 2 shown in Fig. 2a corresponds to "high" loads, while scheme No. 3 in Fig. 2b refers to "superhigh" loads. In all deformation schemes, the normal to the curve l directed inward the area occupied by the plate falls either onto the hinge l_1 or onto the contour l_2, which is the contour of the region Z_p. We use Z_i to denote the region of the plate (not including the region Z_p) with the normals to the contour l from all points of this region falling onto the curve l_i ($i = 1, 2$). We can demonstrate that the normal to the line l_2 is also the normal to the contour l, and the distance D between l and l_2 is independent of the parameter ν_2 [2, 4]. The equation for

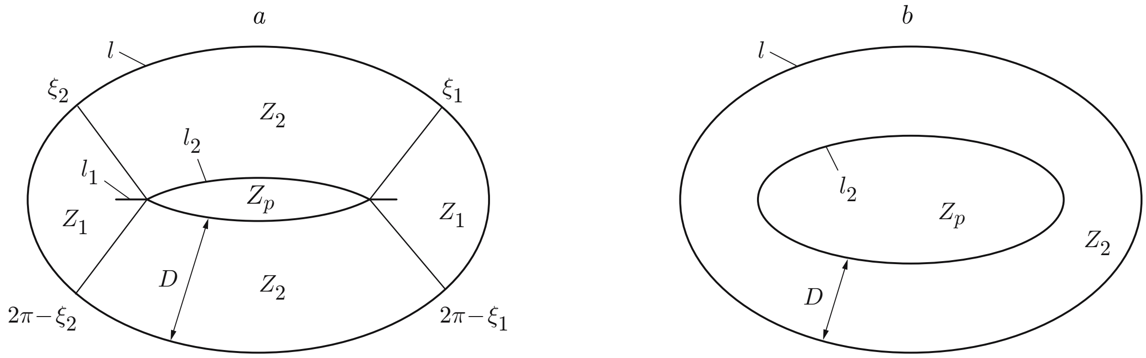

Fig. 2. Deformation scheme Nos. 2 (a) and 3 (b).

the contour l_2 of the region Z_p has the form $\nu_1 = D$ ($\xi_1 \leqslant \nu_2 \leqslant \xi_2$ and $2\pi - \xi_2 \leqslant \nu_2 \leqslant 2\pi - \xi_1$) [2, 4]. The region of constant thickness of the plate ($\nu_1 \geqslant \nu_1^c$) should include the region Z_p. The plate thickness in the region Z_p is denoted by $h(\nu_1) = h_c$. The line l_2 is a plastic hinge with a normal bending moment $\sigma_0 h_c^2/4$.

Scheme No. 2 refers to the general case of plate deformation. If there are no regions Z_p and Z_2, this scheme coincides with scheme No. 1. If there is no region Z_1, scheme No. 2 transforms to scheme No. 3. Let us consider scheme No. 2.

The equation of motion of the plate is derived from the principle of virtual power with the use of the d'Alembert principle [15]:

$$K = A - N. \tag{2}$$

Here K and A are the powers of inertial and external forces, respectively,

$$K = \iiint\limits_V \rho_V \ddot{u}\dot{u}^*\, dV, \qquad A = \iint\limits_S P(t)\dot{u}^*\, dS,$$

N is the power of internal forces, V and S are the volume and area of the plate, ρ_V is the density of the plate material, u is the deflection, and dV and dS are the volume and area elements; the dots over the symbols denote the derivatives with respect to time; the quantities marked by the asterisk are admissible velocities. The expression for N is written below.

We use $\dot{w}_c(t)$ to denote the velocity of translational motion of the region Z_p and $\dot{\alpha}$ to denote the velocity of the angle of turning of the region Z_2 on the support contour. The condition of continuity of velocities on the boundary between the regions Z_2 and Z_p implies that $\dot{\alpha}$ is independent of the parameter ν_2. Because of continuity of velocities on the boundaries between the regions Z_1 and Z_2, like in [8], the velocity of the angle of turning of the region Z_1 on the support contour is also $\dot{\alpha}$. Then, the deflection rates of the plate are

$$(\nu_1, \nu_2) \in Z_p\colon \quad \dot{u}(\nu_1, \nu_2, t) = \dot{w}_c(t), \qquad (\nu_1, \nu_2) \in Z_i\colon \quad \dot{u}(\nu_1, \nu_2, t) = \dot{\alpha}(t)\nu_1 \qquad (i = 1, 2). \tag{3}$$

The main curvatures of the surface of deflection rates of the plate in the regions Z_1 and Z_2 are

$$\kappa_1 = \frac{\partial^2 \dot{u}}{\partial \nu_1^2} = 0, \qquad \kappa_2 = \frac{1}{\rho_1}\frac{\partial \dot{u}}{\partial \nu_1} = \frac{\dot{\alpha}(t)}{R(\nu_2) - \nu_1}.$$

In the regions Z_1 and Z_2, the bending moment is $M_{22} = \sigma_0 h^2(\nu_1)/4$. On the contour l of the plate, we have $u(0, \nu_2, t) = \dot{u}(0, \nu_2, t) = 0$ and $M_{11} = -\sigma_0 h^2(0)(1 - \eta)/4$, where $\eta = 0$ if the contour l is clamped and $\eta = 1$ if it is simply supported.

Taking into account the distribution of deflection rates (3) and the fact that the condition $h(\nu_1) = h_c$ is satisfied in the region Z_p, with $dV = h(\nu_1)\, ds$ and $ds = L(1 - \nu_1/R)\, d\nu_1\, d\nu_2$, we obtain

$$K = \rho_V\Big(\ddot{\alpha}\dot{\alpha}^* \iint\limits_{Z_1\cup Z_2} h(\nu_1)\nu_1^2\, ds + \ddot{w}_c\dot{w}_c^* \iint\limits_{Z_p} h\, ds\Big) = \rho_V\Big(\ddot{\alpha}\dot{\alpha}^*\Sigma_1 + \ddot{w}_c\dot{w}_c^* h_c \iint\limits_{Z_p} ds\Big),$$

$$A = P(t)\Big(\dot{\alpha}^* \iint\limits_{Z_1\cup Z_2} \nu_1\, ds + \dot{w}_c^* \iint\limits_{Z_p} ds\Big) = P(t)\Big(\dot{\alpha}^*\Sigma_2 + \dot{w}_c^* \iint\limits_{Z_p} ds\Big),$$

$$\Sigma_1(\xi_1,\xi_2,D) = 2\Big\{ \int\limits_0^{\xi_1} L\Big[\int\limits_0^{D_l(\nu_2)} h\nu_1^2\Big(1-\frac{\nu_1}{R}\Big)\,d\nu_1\Big]\,d\nu_2$$

$$+ \int\limits_{\xi_1}^{\xi_2} L\Big[\int\limits_0^{D(t)} h\nu_1^2\Big(1-\frac{\nu_1}{R}\Big)d\nu_1\Big]\,d\nu_2 + \int\limits_{\xi_2}^{\pi} L\Big[\int\limits_0^{D_l(\nu_2)} h\nu_1^2\Big(1-\frac{\nu_1}{R}\Big)\,d\nu_1\Big]\,d\nu_2\Big\},$$

$$\Sigma_2(\xi_1,\xi_2,D) = 2\Big\{ \int\limits_0^{\xi_1} L\Big[\int\limits_0^{D_l(\nu_2)} \nu_1\Big(1-\frac{\nu_1}{R}\Big)\,d\nu_1\Big]\,d\nu_2$$

$$+ \int\limits_{\xi_1}^{\xi_2} L\Big[\int\limits_0^{D(t)} \nu_1\Big(1-\frac{\nu_1}{R}\Big)\,d\nu_1\Big]\,d\nu_2 + \int\limits_{\xi_2}^{\pi} L\Big[\int\limits_0^{D_l(\nu_2)} \nu_1\Big(1-\frac{\nu_1}{R}\Big)\,d\nu_1\Big]\,d\nu_2\Big\}.$$

The expression for the power of internal forces N in Eq. (2) is presented as

$$N = \sum_{i=1}^{4} N_i,$$

where N_1, N_2, N_3, and N_4 are the powers of internal forces on the contour l, inside the regions Z_1 and Z_2, on the line l_2, and on the line l_1, respectively,

$$N_1 = (1-\eta)\sigma_0\,\frac{h^2(0)}{4}\oint\limits_l [\dot\theta^*]_l\,dl \quad (dl = L\,d\nu_2), \qquad N_2 = \frac{\sigma_0}{4}\iint\limits_{Z_1\cup Z_2} h^2(\nu_1)\kappa_2^*\,ds,$$

$$N_3 = \sigma_0\,\frac{h^2(D)}{4}\oint\limits_{l_2}[\dot\theta^*]_{l_2}\,dl_2, \qquad N_4 = \frac{\sigma_0}{4}\int\limits_{l_1} h^2(D_l(\nu_2))[\dot\theta^*]_{l_1}\,dl_1,$$

$[\dot\theta]_m$ is the discontinuity of the angular velocity on the line m, and dl, dl_1, and dl_2 are the length elements of the lines l, l_1, and l_2. With allowance for the fact that the normal to the line l_2 is also the normal to the contour l, Eq. (3) implies that $[\dot\theta]_l = [\dot\theta]_{l_2} = \dot\alpha$. Then, we obtain

$$N_1 = (1-\eta)\sigma_0\,\frac{h^2(0)}{2}\,\dot\alpha^*\int\limits_0^{\pi} L\,d\nu_2,$$

$$N_2 = \frac{\sigma_0}{4}\,\dot\alpha^*\iint\limits_{Z_1\cup Z_2} h^2(\nu_1)\,\frac{1}{R(\nu_2)-\nu_1}\,ds$$

$$= \frac{\sigma_0}{2}\,\dot\alpha^*\Big[\int\limits_0^{\xi_1}\frac{L}{R}\Big(\int\limits_0^{D_l(\nu_2)} h^2\,d\nu_1\Big)\,d\nu_2 + \Big(\int\limits_{\xi_1}^{\xi_2}\frac{L}{R}\,d\nu_2\Big)\int\limits_0^{D(t)} h^2\,d\nu_1 + \int\limits_{\xi_2}^{\pi}\frac{L}{R}\Big(\int\limits_0^{D_l(\nu_2)} h^2\,d\nu_1\Big)\,d\nu_2\Big],$$

$$N_3 = \sigma_0\,\frac{h^2(D)}{4}\,\dot\alpha^*\int\limits_{l_2} dl_2 = \frac{\sigma_0}{2}\,h^2(D)\dot\alpha^*\int\limits_{\xi_1}^{\xi_2} L\Big(1-\frac{D}{R}\Big)\,d\nu_2.$$

To determine N_4, we calculate $[\dot\theta]_{l_1}$ and dl_1. From Eq. (1), for the line l_1 we obtain $dl_1 = \sqrt{(1-D_l/R)^2L^2 + (\partial D_l/\partial\nu_2)^2}\,d\nu_2$. As $(\partial D_l/\partial\nu_2)^2 = (y_1'^2L^2/x_1'^2)(1-D_l/R)^2$, then

$$dl_1 = \frac{(1-D_l/R)L^2}{|x_1'|}\,d\nu_2.$$

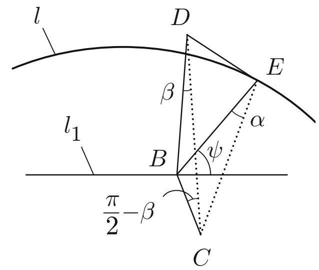

Fig. 3. Additional plot for calculating the discontinuity of the angular velocity on the line l_1.

The discontinuity of the angular velocity on the line l_1 is denoted by $[\dot{\theta}]_{l_1} = 2\dot{\beta}$. To calculate the angle β, from the point $E(0, \nu_2)$ of the contour l, such that $\nu_2 \in (0, \xi_1)$ or $\nu_2 \in (\xi_2, \pi)$, on an undeformed plate we plot the normal to l until its intersection with the line l_1 at the point B (Figs. 1 and 3); $|BE| = D_l(\nu_2)$. The segment BE intersects the line l_1 at an angle ψ ($\tan\psi = -x_1'/y_1'$). Through the segment BE, we plot the plane BEC perpendicular to the original surface of the plate ($BC \perp BE$) (see Fig. 3). We also plot the plane ECD tangential to the deformed plate surface along the straight line EC. Then, we have $\angle BEC = \alpha$. Through the point B, we plot the plane BCD normal to the line l_1. We obtain $\angle BCD = \pi/2 - \beta$ and, hence, $\angle BDC = \beta$. As $|BC| = |BE|\,\alpha$ and $|BC| = |BD|\,\beta$, we have $\beta = \alpha\,|BE|/|BD|$. Then, we obtain

$$\dot{\beta} = \dot{\alpha}\sin\psi = \dot{\alpha}|x_1'|/L.$$

Substituting the calculated values into the expression for N_4, we obtain

$$N_4 = \dot{\alpha}^* \frac{\sigma_0}{2}\Big[\int\limits_0^{\xi_1} h^2(D_l(\nu_2))\Big(1 - \frac{D_l}{R}\Big) L\,d\nu_2 + \int\limits_{\xi_2}^{\pi} h^2(D_l(\nu_2))\Big(1 - \frac{D_l}{R}\Big) L\,d\nu_2\Big].$$

The total power of internal forces of the plate N is described by the expression

$$N = \dot{\alpha}^*\sigma_0\Sigma_3, \qquad \Sigma_3(\xi_1, \xi_2, D) = \frac{1}{\dot{\alpha}^*\sigma_0}\sum_{i=1}^{4} N_i.$$

Note, if $h(\nu_1) = \mathrm{const}$, then

$$N = (2-\eta)\dot{\alpha}^*\sigma_0\frac{h^2}{4}\int\limits_0^{2\pi} L\,d\nu_2.$$

Substituting the expressions for K, A, and N into Eq. (2) and taking into account that $\dot{\alpha}^*$ and $\dot{w}_c^*$ are independent of each other, we obtain the equations of motion in the case of deformation by scheme No. 2:

$$\rho_V\ddot{\alpha}\Sigma_1 = P(t)\Sigma_2 - \sigma_0\Sigma_3; \tag{4}$$

$$\rho_V h_c\ddot{w}_c = P(t). \tag{5}$$

The condition of continuity of velocities on the boundaries between the regions Z_2 and Z_p, Z_2 and Z_1 implies that

$$\dot{\alpha}D = \dot{w}_c; \tag{6}$$

$$D(t) = D_l(\xi_i(t)) \qquad (i = 1, 2). \tag{7}$$

The initial conditions are

$$\dot{\alpha}(0) = \alpha(0) = \dot{w}_c(0) = w_c(0) = 0. \tag{8}$$

The initial values of $D_0 = D(0)$ and $\xi_{i0} = \xi_i(0)$ for the functions $D(t)$ and $\xi_i(t)$ $(i = 1, 2)$ are determined, depending on the value of $P_{\max}$ (see below).

System (4)–(7) describes the plate motion in the case of its deformation by scheme No. 2. In the case with scheme No. 3, the region Z_1 is absent, and the motion is described by Eqs. (4)–(6) with Σ_i $(i = 1, \dots, 3)$ substituted by $\Omega_i(D) = \Sigma_i(0, \pi, D)$. In the case with scheme No. 1, the regions Z_2 and Z_p are absent, and the behavior of the plate is described by Eq. (4) with Σ_i $(i = 1, \dots, 3)$ substituted by $\Omega_i^* = \Sigma_i(\xi_m, \xi_m, D_{\max})$, where the value of ξ_m is such that $D_{\max} = \max\limits_{\nu_2} D_l(\nu_2) = D_l(\xi_m)$.

2. Let us analyze plate deformation. If $0 < P_{\max} \leqslant P_0$ ("low" loads), where P_0 is the limit load, the plate remains at rest. We find the value of P_0 from Eq. (4) with Σ_i substituted by Ω_i^* $(i = 1, \dots, 3)$ at the beginning of motion $t = 0$, assuming that $\ddot{\alpha}(0) = 0$. Then, we obtain

$$P_0 = \sigma_0 \Omega_3^* / \Omega_2^*. \tag{9}$$

If $P_0 < P_{\max} \leqslant P_1$ ("medium" loads), where P_1 is the load corresponding to the emergence of the region Z_p, then, the plate motion follows scheme No. 1. The load P_1 is determined as follows. Differentiating Eq. (6) with respect to time and eliminating the quantities $\ddot{\alpha}$ and $\ddot{w}_c$ with the use of Eqs. (4) and (5), we obtain the relation

$$-\frac{\rho_V \dot{\alpha} \dot{D}}{D}\, \Sigma_1 = P(t)\Big(\Sigma_2 - \frac{\Sigma_1}{D h_c}\Big) - \sigma_0 \Sigma_3. \tag{10}$$

When the regions Z_2 and Z_p appear at the time $t = 0$, the region Z_1 occupies the entire plate and $\xi_1 = \xi_2 = \xi_m$ and $D = D_{\max}$. Then, Eq. (10) yields

$$P_1 = \frac{\sigma_0 \Omega_3^*}{\Omega_2^* - \Omega_1^*/(D_{\max} h_c)}. \tag{11}$$

It follows from Eqs. (9) and (11) that $P_0 < P_1$ independent of the form of the function $h(\nu_1)$. In the case with scheme No. 1, the equation of motion (4) can be written as

$$\ddot{\alpha}(t) = F[P(t) - P_0], \qquad F = \Omega_2^*/(\rho_V \Omega_1^*). \tag{12}$$

The initial conditions have the form (8). At the time $t = T$, the load is removed, and the plate moves due to inertia for a certain time.

At $0 \leqslant t \leqslant T$, integration of the equation of motion (12) yields

$$\dot{\alpha}(t) = F\Big(\int_0^t P(\tau)\, d\tau - P_0 t\Big), \qquad \alpha(t) = F\Big(\int_0^t \int_0^\lambda P(\tau)\, d\tau\, d\lambda - P_0 \frac{t^2}{2}\Big).$$

At $T < t \leqslant t_f$, the plate motion is due to inertia until it stops at the time t_f; this motion is described by the equation

$$\ddot{\alpha}(t) = -F P_0$$

with the initial conditions $\dot{\alpha}(T)$ and $\alpha(T)$. The final time t_f is found from the condition

$$\dot{\alpha}(t_f) = 0. \tag{13}$$

Integrating the equation of motion, we obtain the equalities

$$\dot{\alpha}(t) = \dot{\alpha}(T) - F P_0 (t - T); \tag{14}$$

$$\alpha(t) = \alpha(T) + \dot{\alpha}(T)(t - T) - F P_0 (t - T)^2/2.$$

It follows from Eqs. (13) and (14) that

$$t_f = \frac{1}{P_0} \int_0^T P(t)\, dt.$$

The deflection is calculated by Eqs. (3), and the maximum final deflection is found by the formula

$$u_{\max} = D_{\max} F \Big[\frac{1}{2P_0}\Big(\int_0^T P(t)\, dt\Big)^2 - \int_0^T t P(t)\, dt\Big]. \tag{15}$$

If $P_1 < P_{\max} \leqslant P_2$ ("high" loads), where P_2 is the load at which the region Z_1 and the hinge l_1 disappear, the motion begins with a developed region Z_p at $D_{\min} < D_0 < D_{\max}$, where $D_{\min} = \min\limits_{\nu_2} D_l(\nu_2) = \min(D_l(0), D_l(\pi))$.

For plates with a smooth support contour, $D_{\min} = \min(R(0), R(\pi))$. The initial values of D_0 and ξ_{i0} are determined by equalities (7) and Eq. (10) with allowance for the condition $\dot\alpha(0) = 0$:

$$P_{\max}\Big(\Sigma_2(\xi_{10}, \xi_{20}, D_0) - \frac{\Sigma_1(\xi_{10}, \xi_{20}, D_0)}{D_0 h_c}\Big) = \sigma_0 \Sigma_3(\xi_{10}, \xi_{20}, D_0). \tag{16}$$

For plates with singular points on the contour, the hinge l_1 does not disappear and $D_{\min} = 0$; in this case, the load P_2 cannot be determined. For plates with a smooth contour l, the load P_2 is determined from Eq. (16) with $D = D_{\min}$, $\xi_1 = 0$, and $\xi_2 = \pi$:

$$P_2 = \frac{\sigma_0 \Sigma_3(0, \pi, D_{\min})}{\Sigma_2(0, \pi, D_{\min}) - \Sigma_1(0, \pi, D_{\min})/(D_{\min} h_c)}.$$

In the first phase of deformation ($0 < t \leqslant t_1$), the plate motion follows scheme No. 2 and is described by Eqs. (4)–(7) with the initial conditions (8) and (16). In this phase, the size of the region Z_p decreases by the law described by Eq. (10) ($\dot D > 0$). The time t_1 corresponding to disappearance of the region Z_p is determined from the equality $D(t_1) = D_{\max}$, with $\xi_1(t_1) = \xi_2(t_1) = \xi_m$. At this moment, the values of $\dot\alpha(t_1)$, $\alpha(t_1)$, $\dot w_c(t_1)$, and $w_c(t_1)$ are determined. In this phase, the motion can cease at $D(t_{1f}) < D_{\max}$ at the time t_{1f} determined from the equation $\dot\alpha(t_{1f}) = 0$. If $t_1 < t_{1f}$, then the motion continues in the second phase.

The second phase of plate motion ($t_1 < t \leqslant t_f$) follows scheme No. 1 until termination at the time t_f. Plate deformation is described by Eq. (12) with the initial conditions determined at the end of the first phase of motion. The final time is found from condition (13). All deflections of the plate are calculated from Eqs. (3) with allowance for all phases of motion.

If $P_{\max} > P_2$ ("superhigh" loads), then the plate motion begins in accordance with scheme No. 3 with a developed region Z_p. The value of D_0 is found from Eq. (10) with Σ_i substituted by $\Omega_i(D_0)$ ($i = 1, \ldots, 3$) with allowance for the condition $\dot\alpha(0) = 0$:

$$P_{\max}(\Omega_2(D_0) - \Omega_1(D_0)/(D_0 h_c)) = \sigma_0 \Omega_3(D_0). \tag{17}$$

In the first phase of deformation ($0 < t \leqslant t_1$), the plate motion follows scheme No. 3 and is described by Eqs. (4)–(6) with Σ_i substituted by $\Omega_i(D)$ ($i = 1, \ldots, 3$) with the initial conditions (8) and (17). In this phase, the size of the region Z_p decreases in accordance with the law described by Eq. (10) with Σ_i substituted by $\Omega_i(D)$. The time t_1 corresponding to the emergence of the region Z_2 is determined from the equality $D(t_1) = D_{\min}$. At this moment, the values of $\dot\alpha(t_1)$, $\alpha(t_1)$, $\dot w_c(t_1)$, $w_c(t_1)$, $\xi_1(t_1) = 0$, and $\xi_2(t_1) = \pi$ are found. In this phase, the motion can cease at $D(t_{2f}) < D_{\min}$ at the time t_{2f} determined from the equation $\dot\alpha(t_{2f}) = 0$. If $t_1 < t_{1f}$, the motion continues in the second phase.

The motion in the second ($t_1 < t \leqslant t_2$) and third ($t_2 < t \leqslant t_f$) phases is similar to the motion in the first and second phases of deformation in the case of "high" loads with appropriate initial values. All deflections are calculated by Eqs. (3) with allowance for all phases of motion.

3. Let us consider the restrictions imposed onto the function $h(\nu_1)$ and on the value of $P_{\max}$ in the deformation scheme proposed. These conditions are obtained by comparing the limit load P_0 with the limit load in other possible schemes of motion. If the value of h_c is sufficiently large, then the bending moment $M_{22} = \sigma_0 h_c^2/4$ in a certain central region Z_c ($\nu_1^c \leqslant \nu_1 \leqslant D_l(\nu_2)$, where $0 \leqslant \nu_2 \leqslant 2\pi$ ($\nu_1^c \leqslant D_{\min}$) or $\xi_1^c \leqslant \nu_2 \leqslant \xi_2^c$ and $2\pi - \xi_2^c \leqslant \nu_2 \leqslant 2\pi - \xi_1^c$ ($\nu_1^c > D_{\min}$)) is substantially greater than that in the remaining part of the plate. Hence, the region Z_c is not deformed, and the plate motion occurs in the presence of the rigid central region Z_c moving translationally with a velocity $\dot\alpha\nu_1^c$. Let us find the limit load P_0^c for such a deformation scheme. The power of external forces A^c is

$$A^c = P(t)\Big(\iint\limits_{Z_1\cup Z_2} \dot\alpha^* \nu_1\, ds + \iint\limits_{Z_c} \dot\alpha^* \nu_1^c\, ds\Big) = P(t)\dot\alpha^* \Sigma_2^c,$$

$$\Sigma_2^c(\xi_1^c, \xi_2^c, \nu_1^c) = 2\Big\{\int\limits_0^{\xi_1^c} L\Big[\int\limits_0^{D_l(\nu_2)} \nu_1\Big(1 - \frac{\nu_1}{R}\Big)\, d\nu_1\Big]\, d\nu_2 + \int\limits_{\xi_1^c}^{\xi_2^c} L\Big[\int\limits_0^{\nu_1^c} \nu_1\Big(1 - \frac{\nu_1}{R}\Big)\, d\nu_1\Big]\, d\nu_2$$
$$+ \int\limits_{\xi_2^c}^{\pi} L\Big[\int\limits_0^{D_l(\nu_2)} \nu_1\Big(1 - \frac{\nu_1}{R}\Big)\, d\nu_1\Big]\, d\nu_2 + \nu_1^c \int\limits_{\xi_1^c}^{\xi_2^c} L\Big[\int\limits_{\nu_1^c}^{D_l(\nu_2)} \Big(1 - \frac{\nu_1}{R}\Big)\, d\nu_1\Big]\, d\nu_2\Big\}.$$

Then, we have $P_0^c = \sigma_0 \Sigma_3(\xi_1^c, \xi_2^c, \nu_1^c)/\Sigma_2^c(\xi_1^c, \xi_2^c, \nu_1^c)$.

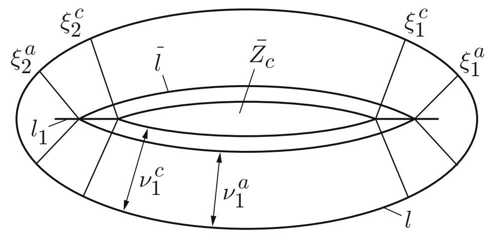

Fig. 4. Scheme No. 1 of plate deformation in the case where the central part of the plate $\bar{Z}_c$ $[\nu_1^c \leqslant \nu_1 \leqslant D_l(\nu_2)]$ remains rigid simultaneously with formation of the boundary hinge $\bar{l}$ $(\nu_1 = \nu_1^a)$.

Plates of variable thickness may deform with formation of boundary plastic hinges $\bar{l}$ at a certain distance ν_1^a from the contour l inside the plate rather than over the perimeter of the support contour; in this case, the region near the plate contour remains undeformed. The equation of the contour $\bar{l}$ has the form $\nu_1 = \nu_1^a$ ($\xi_1^a \leqslant \nu_2 \leqslant \xi_2^a$ and $2\pi - \xi_2^a \leqslant \nu_2 \leqslant 2\pi - \xi_1^a$). On the contour $\bar{l}$, the bending moment is $M_{11} = -\sigma_0 h^2(\nu_1^a)/4$. It follows from Eq. (9) that the limit load $\bar{P}_0$ for a clamped curvilinear plate with the contour $\bar{l}$ is

$$\bar{P}_0 = \sigma_0 \bar{\Omega}_3 / \bar{\Omega}_2,$$

where

$$\bar{\Omega}_3(\xi_1^a, \xi_2^a, \nu_1^a) = \frac{1}{2}\Big[h^2(\nu_1^a)\int\limits_{\xi_1^a}^{\xi_2^a} L\Big(1 - \frac{\nu_1^a}{R}\Big)\,d\nu_2 + \int\limits_{\xi_1^a}^{\xi_2^a} \frac{L}{R}\Big(\int\limits_{\nu_1^a}^{D_l(\nu_2)} h^2\,d\nu_1\Big)d\nu_2 + \int\limits_{\xi_1^a}^{\xi_2^a} h^2(D_l(\nu_2))\Big(1 - \frac{D_l}{R}\Big)\,d\nu_2\Big],$$

$$\bar{\Omega}_2(\xi_1^a, \xi_2^a, \nu_1^a) = 2\int\limits_{\xi_1^a}^{\xi_2^a} L\Big[\int\limits_{\nu_1^a}^{D_l(\nu_2)} (\nu_1 - \nu_1^a)\Big(1 - \frac{\nu_1}{R}\Big)\,d\nu_1\Big]d\nu_2.$$

In this case, a situation is also possible where some central part of the plate $\bar{Z}_c$ $(\nu_1^c \leqslant \nu_1 \leqslant D_l(\nu_2))$ remains rigid, in addition to formation of the boundary hinge $\bar{l}$ $(\nu_1 = \nu_1^a)$ (Fig. 4). Let us determine the limit load $\bar{P}_0^c$ for such a deformation scheme. The power of external forces $\bar{A}^c$ is

$$\bar{A}^c = P(t)\Big(\iint\limits_{\bar{Z}_1 \cup \bar{Z}_2} \dot{\alpha}^* \nu_1\,ds + \iint\limits_{\bar{Z}_c} \dot{\alpha}^* \nu_1^c\,ds\Big) = P(t)\dot{\alpha}^* \bar{\Sigma}_2^c,$$

$$\bar{\Sigma}_2^c(\xi_1^c, \xi_2^c, \nu_1^c) = 2\Big\{\int\limits_{\xi_1^a}^{\xi_1^c} L\Big[\int\limits_{\nu_1^a}^{D_l(\nu_2)} (\nu_1 - \nu_1^a)\Big(1 - \frac{\nu_1}{R}\Big)\,d\nu_1\Big]\,d\nu_2$$

$$+ \int\limits_{\xi_1^c}^{\xi_2^c} L\Big[\int\limits_{\nu_1^a}^{\nu_1^c} (\nu_1 - \nu_1^a)\Big(1 - \frac{\nu_1}{R}\Big)\,d\nu_1\Big]\,d\nu_2 + \int\limits_{\xi_2^c}^{\xi_2^a} L\Big[\int\limits_{\nu_1^a}^{D_l(\nu_2)} (\nu_1 - \nu_1^a)\Big(1 - \frac{\nu_1}{R}\Big)\,d\nu_1\Big]\,d\nu_2 + \nu_1^c \int\limits_{\xi_1^c}^{\xi_2^c} L\Big[\int\limits_{\nu_1^c}^{D_l(\nu_2)} \Big(1 - \frac{\nu_1}{R}\Big)\,d\nu_1\Big]\,d\nu_2\Big\}.$$

Then, we have $\bar{P}_0^c = \sigma_0 \bar{\Omega}_3(\xi_1^a, \xi_2^a, \nu_1^a)/\bar{\Sigma}_2^c(\xi_1^c, \xi_2^c, \nu_1^c)$.

If the function $h(\nu_1)$ has such a form that the inequality $P_0 < \min(P_0^c, \bar{P}_0, \bar{P}_0^c)$ is valid, the plate deformation occurs in accordance with scheme Nos. 1–3 (see Secs. 1 and 2). As the model of motion proposed was derived under the assumption that $h(\nu_1) = \text{const} = h_c$ in the region Z_p, it follows from Eqs. (16) and (17) that there are restrictions on the value of $P_{\max}$:

$$P_{\max} \leqslant \frac{\sigma_0 \Omega_3(\nu_1^c)}{\Omega_2(\nu_1^c) - \Omega_1(\nu_1^c)/(\nu_1^c h_c)}$$

for plates with a smooth contour l and

$$P_{\max} \leqslant \frac{\sigma_0 \Sigma_3(\xi_1^c, \xi_2^c, \nu_1^c)}{\Sigma_2(\xi_1^c, \xi_2^c, \nu_1^c) - \Sigma_1(\xi_1^c, \xi_2^c, \nu_1^c)/(\nu_1^c h_c)}$$

for contours with singular points. In these expressions, the values of ξ_i^c ($i = 1, 2$, $\xi_1^c \leqslant \xi_2^c$) are determined by the equality $\nu_1^c = D_l(\xi_i^c)$. For constant-thickness plates, the model is applicable for all values of $P_{\max}$. For loads with $P_{\max} \leqslant P_1$, the model is valid for all functions $h(\nu_1)$, and deformation follows scheme No. 1.

If the function $h(\nu_1)$ and the constants h_c and ν_1^c are such that $P_0^c < \min(P_0, \bar{P}_0, \bar{P}_0^c)$, we have to consider the problem of motion of a variable-thickness curvilinear plate with a rigid insert in the central part of the plate. For $h(\nu_1) = \text{const}$ with $0 \leqslant \nu_1 \leqslant \nu_1^c$, this problem was considered in detail in [16].

If the condition

$$\bar{P}_0 < \min(P_0, P_0^c, \bar{P}_0^c) \tag{18}$$

is satisfied, the plate is deformed only in the central region with the contour $\bar{l}$ ($\nu_1 = \nu_1^a$). The value of ν_1^a corresponds to the minimum value of $\bar{P}_0$ for which inequality (18) holds, and the values of ξ_i^a are determined by the equality $\nu_1^a = D_l(\xi_i^a)$ ($i = 1, 2$, $\xi_1^a \leqslant \xi_2^a$) if the contour $\bar{l}$ passes through the line l_1 or $\xi_1^a = 0$, $\xi_2^a = \pi$ if the contour $\bar{l}$ envelops the line l_1 (these cases correspond to Fig. 2 with $D = \nu_1^a$ and l replaced by $\bar{l}$). In the case considered, the behavior of the plate is qualitatively similar to the behavior studied in Sec. 2, with the contour l replaced by the clamped contour $\bar{l}$.

4. As an example, let us consider the dynamic behavior of a plate with a contour consisting of two arcs of a circumference of radius R with a central angle 2γ (see Fig. 1b). For such a plate, in the polar coordinate system ($r = R - \nu_1$, $\varphi = \nu_2$), we obtain $L = R$, $D_l(\varphi) = R[1 - \cos\gamma/\cos(\gamma - \varphi)]$, and $D_{\max} = D_l(\gamma) = R(1 - \cos\gamma)$ ($0 \leqslant \varphi \leqslant \gamma$ and $0 < \gamma \leqslant \pi/2$). Depending on the value of $P_{\max}$, two mechanisms of deformation of such a plate are possible. Under "medium" loads, the plate surface is deformed into a cone-shaped surface (scheme No. 1). Under "high" loads, a translationally moving region Z_p is formed in the central part of the plate. The contour of the region Z_p consists of two arcs of a circumference of radius $R - D$ with a central angle $2(\gamma - \xi_D)$, where $0 < \xi_D \leqslant \gamma$. For $\xi_D = \gamma$, there are no regions Z_p and Z_2. We assume that $h = h(r)$. In the case with scheme No. 2, the equations of motion of such a plate have the form (4)–(7), where

$$\xi_1 = \xi_D, \qquad \xi_2 = \pi - \xi_D,$$

$$\Sigma_1(\xi_D) = 4\Big\{\int\limits_0^{\xi_D}\Big[\int\limits_{\frac{R\cos\gamma}{\cos(\gamma-\varphi)}}^{R} hr(R-r)^2\,dr\Big]\,d\varphi + (\gamma - \xi_D)\int\limits_{\frac{R\cos\gamma}{\cos(\gamma-\xi_D)}}^{R} hr(R-r)^2\,dr\Big\},$$

$$\Sigma_2(\xi_D) = \frac{2R^3}{3}\Big\{\xi_D - \cos^2\gamma[2\tan\gamma - 3\tan(\gamma - \xi_D)]$$

$$+ \cos^3\gamma\Big(\ln\frac{\cos\gamma[1 - \sin(\gamma - \xi_D)]}{\cos(\gamma - \xi_D)(1 - \sin\gamma)} - \frac{\tan(\gamma - \xi_D)}{\cos(\gamma - \xi_D)}\Big)$$

$$+ (\gamma - \xi_D)\Big(1 - \frac{\cos\gamma}{\cos(\gamma - \xi_D)}\Big)^2\Big(1 + \frac{2\cos\gamma}{\cos(\gamma - \xi_D)}\Big)\Big\},$$

$$\Sigma_3(\xi_D) = (1 - \eta)h^2(R)\gamma R + \int\limits_0^{\xi_D}\Big(\int\limits_{\frac{R\cos\gamma}{\cos(\gamma-\varphi)}}^{R} h^2(r)\,dr\Big)d\varphi$$

$$+ (\gamma - \xi_D)\Big[\int\limits_{\frac{R\cos\gamma}{\cos(\gamma-\xi_D)}}^{R} h^2(r)\,dr + h^2\Big(\frac{R\cos\gamma}{\cos(\gamma - \xi_D)}\Big)\frac{R\cos\gamma}{\cos(\gamma - \xi_D)}\Big]$$

$$+ R\cos\gamma\int\limits_0^{\xi_D} h^2\Big(\frac{R\cos\gamma}{\cos(\gamma - \varphi)}\Big)\frac{d\varphi}{\cos(\gamma - \varphi)}.$$

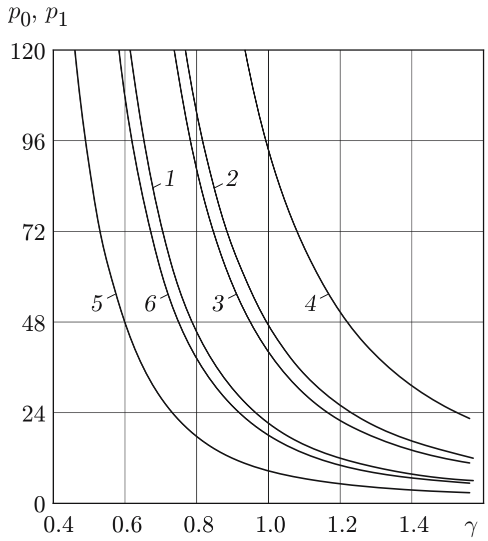

Fig. 5

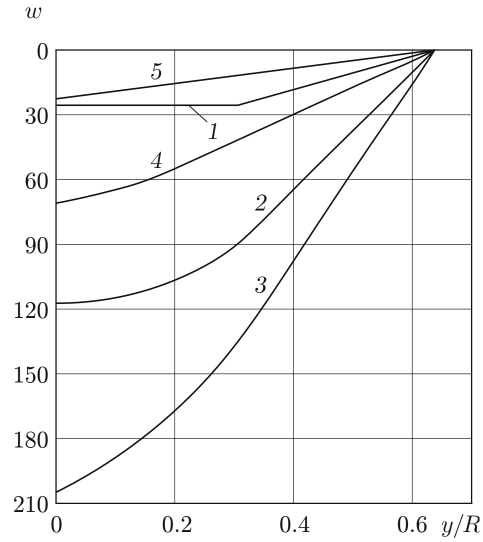

Fig. 6

Fig. 5. Dimensionless limit load p_0 (curves 1, 3, and 5) and load p_1 (curves 2, 4, and 6) versus the angle γ: constant-thickness plate $h(r) = h(R)$ (1 and 2), plate thickness varied by law (19) (3 and 4), and plate thickness varied by law (20) (5 and 6).

Fig. 6. Dimensionless deflections w in the cross section $x = 0$ of a simply supported plate with a contour consisting of two arcs of a circumference of radius R with a central angle 2γ ($\gamma = 1.2$ and $D_{\max} = 0.638R$) under a load in the form of a rectangular pulse: deflection for plate thickness varied by law (20) for $t = T$ (curve 1), $t = t_1 = 2.79T$ (curve 2), and $t = t_f = 6.2T$ (curve 3); curves 4 and 5 refer to the final deflections of a constant-thickness plate $h(r) = h(R)$ ($t_f = 3.22T$) and of a plate with thickness varied by law (19) ($t_f = 1.8T$), respectively.

Figure 5 shows the limit load p_0 and the load p_1 versus the angle γ [$p_i = P_i R^2/M_0$, $i = 0, 1$, and $M_0 = \sigma_0 h^2(R)/4$], which were calculated by Eqs. (9) and (11) for a simply supported plate ($\eta = 1$). Curves 1 and 2 refer to p_0 and p_1 with $h(r) = h(R)$. Curves 3 (for p_0) and 4 (for p_1) correspond to the case

$$h(r) = \begin{cases} h(R)[1 + (R - r)/(2D_{\max})], & R \leqslant r \leqslant R - D_{\max}/2, \\ 5h(R)/4, & R - D_{\max}/2 \leqslant r \leqslant R\cos\gamma, \end{cases} \tag{19}$$

and curves 5 (for p_0) and 6 (for p_1) refer to the case

$$h(r) = \begin{cases} h(R)[1 - (R - r)/(2D_{\max})], & R \leqslant r \leqslant R - D_{\max}/2, \\ 3h(R)/4, & R - D_{\max}/2 \leqslant r \leqslant R\cos\gamma. \end{cases} \tag{20}$$

The deflections $w = uR^2\rho_V h(R)/(M_0T^2)$ of the simply supported plate with $\gamma = 1, 2$, $D_{\max} = 0.638R$ in the cross section $x = 0$ are plotted in Fig. 6. The plate is subjected to loading in the form of a rectangular pulse: $P(t) = 38.37M_0/R^2$ at $0 \leqslant t \leqslant T$ and $P(t) = 0$ at $t > T$. Curves 1–3 show the deflections with plate thickness varied by law (20) at the times $t = T$, $t = t_1 = 2.79T$, and $t = t_f = 6.2T$, respectively [$\xi_D(0) = 0.2$]. Curve 4 shows the final deflection of the plate considered in the case $h(r) = h(R)$ ($t_f = 3.22T$). If plate thickness varies by law (19), plate deformation follows the scheme for "medium" loads, because $P_0 = 21.34M_0/R^2$ and $P_1 = 50.58M_0/R^2 > P_{\max}$. At $t_f = 1.8T$, the maximum final deflection at the plate center, calculated by Eq. (15), is $w = 21.16$ (curve 5).

It follows from Figs. 5 and 6 that a change in plate thickness produces a significant effect both on the magnitude of the limit load and on the final deflections. For loads higher than the limit values, the limit load may be increased severalfold and the final deflection may be reduced by changing the plate thickness, thus, the quality of the structure is improved.

This work was supported by the Russian Foundation for Basic Research (Grant No. 06-08-08035-ofi).

REFERENCES

1. K. L. Komarov and Yu. V. Nemirovsky, *Dynamics of Rigid-Plastic Structural Elements* [in Russian], Nauka, Novosibirsk (1984).
2. Yu. V. Nemirovsky and T. P. Romanova, "Dynamics of plastic deformation of curvilinear plates," *Int. Appl. Mech.*, **37**, No. 12, 1568–1578 (2001).
3. Yu. V. Nemirovsky and T. P. Romanova, "Plastic deformation of doubly connected plates with a curvilinear contour under dynamic loads," in: *Urgent Problems of Dynamics and Strength in Theoretical and Applied Mechanics* [in Russian], Tekhnoprint, Minsk (2001), pp. 515–525.
4. Yu. V. Nemirovsky and T. P. Romanova, "Dynamic plastic damage of simply and doubly connected elliptic plates," *J. Appl. Mech. Tech. Phys.*, **43**, No. 2, 291–301 (2002).
5. Yu. V. Nemirovsky and T. P. Romanova, "Modeling and analysis of forging of thin-walled structures with smooth convex contours," in: *Mechanics of Shells and Plates*, Proc. of the 20th Int. Conf. on the Theory of Shells and Plates (Nizhnii Novgorod, September 17–19, 2002), Izd. Nizhegor. Univ., Nizhnii Novgorod (2002), pp. 231–239.
6. Yu. V. Nemirovsky and T. P. Romanova, "Damage of plane targets with non-concave contours under explosive loading," *Nauch. Vestn. Novosib. Gos. Tekh. Univ.*, No. 2, 77–85 (2002).
7. Yu. V. Nemirovsky and T. P. Romanova, "Dynamics of plastic plates in the form of irregular ovals," in: *Urgent Problems of Mechanics and Applied Mathematics* [in Russian], Proc. Int. Workshop (Voronezh, June 4–8, 2002), Part 1, Voronezh State University, Voronezh (2003), pp. 182–196.
8. Yu. V. Nemirovsky and T. P. Romanova, "Dynamic behavior of rigid-plastic sector plates," *Int. Appl. Mech.*, **40**, No. 4, 440–447 (2004).
9. Yu. V. Nemirovsky and T. P. Romanova, "Damage of rigid-plastic doubly connected curvilinear plates in a viscous medium under explosive loads," in: *Science. Industry. Defence*, Proc. 7th All-Russia Conf. (Novosibirsk, April 19–21, 2006), Novosibirsk State Tech. Univ., Novosibirsk (2006), pp. 317–323.
10. M. I. Reitman and G. S. Shapiro, *Methods of Optimal Design of Deformable Solids* [in Russian], Nauka, Moscow (1976).
11. Yu. V. Nemirovsky and V. N. Mazalov (eds.), *Optimal Design: Bibliographic Index* [in Russian], Vol. 1 and 2, Inst. Hydrodynamics, Sib. Div., Acad. of Sci. of the USSR, Novosibirsk (1975).
12. H. Yakimawa, "Design of optimal dynamically loaded structures," in: *Novel Directions in Structural Design* [Russian translation], Stroiizdat, Moscow (1989), pp. 245–262.
13. Yu. V. Nemirovsky, "Optimal design of homogeneous and layered plastic beams under dynamic loading," in: *Proc. 5th All-Russia Workshop* (Novosibirsk, April 7–8, 2005), Novosibirsk State University of Architecture and Civil Engineering, Novosibirsk (2005), pp. 261–267.
14. B. A. Lyukshin and V. A. Kovalev, "Calculation of elastoplastic shells of revolution of variable thickness under dynamic loading," in: T. M. Platova (ed.), *Mechanics of Continuous Media* (collected scientific papers) [in Russian], Izd. Tomsk. Univ., Tomsk (1983), pp. 10–17.
15. M. I. Erkhov, *Theory of Ideal Plastic Solids and Structures* [in Russian], Nauka, Moscow (1978).
16. Yu. V. Nemirovsky and T. P. Romanova, "Dynamic deformation of a curved plate with a rigid insert," *J. Appl. Mech. Tech. Phys.*, **47**, No. 2, 254–265 (2006).